한국동력기계공학회지 제15권 제3호 pp.31~37 2011년 6월

The Effects of Woven Metal Screen Ribs on Heat Transfer and Pressure Drops in the 5:1 Aspect Ratio Rectangular Duct
5:1의 형상비를 갖는 사각덕트에서 직조 스크린 리입(rib)이 열전달과 마찰계수에 미치는 영향

오세경 · 아리바시아 크리시나 부트라 · 안수환 · 이명성
S. K. Oh, B. K. P, Ary, S. W. Ahn and M. S. Lee

(접수일 : 2010년 12월 03일, 수정일 : 2011년 03월 25일, 채택일 : 2011년 04월 20일)

Key Words : 직조 금속 스크린 리입(Woven Metal Screen Rib), 열전달(Heat Transfer), 마찰계수(Friction Factor), 사각 덕트(Rectangular Duct)

Abstract : 직조 금속 스크린 리브(rib)이 바닥에 설치된 사각 덕트에서 열전달과 유체유동의 압력강하를 측정하기 위해 실험적 연구를 수행하였다. 시험부의 치수는 200 mm(W) x 40 mm(H) x 712 mm(L)이고 수력직경은 66.6 mm이다. 입구영역에는 1.72m 길이의 가열되지 않은 동일한 치수의 채널을 설치하였다. 메쉬가 다른 4가지의 직조금속 스크린 리브에 대해 측정하였다. 그리고 비교를 위해 일체형 리브에 대해서도 측정하였다. 국부 열전달 계수의 측정에는 스테인레스 강제 포일(foil) 히터와 T형 열전대를 이용하였다. 레이놀즈 수는 23,000에서 58,000의 범위이다. 덕트의 수력직경(D_h)에 대한 직조 금속 리브의 높이(e)의 비(e/D_h)는 0.075이고 리브 간격(p)과 높이의 비(p/e)는 10이다. 실험 결과 메쉬가 없는 일체형 리입에서 가장 누셀트 수와 마찰계수가 컸다.

1. 서 론

Metallic woven screen meshes have been widely used in refrigeration, chemical reaction, food processing, solar energy collection, heat dissipation, combustion, and refrigeration system for heat transfer enhancements1-5). Due to the large values of surface area density(defined as wetted surface area per volume), these structures are found to be effective in dissipating heat within a limited design space6,7). Much attention has hence been drawn to study the hydraulic and thermal performance of these structures.

Ergun8), Armour and Cannon9) and Sodre and Parise10) experimentally investigated the flow through the woven screen structures with focus placed on hydraulic characteristics. Richards and Robinson4)studied the effect of wire shapes on pressure drop and found that the friction factor depends both on structure porosities and the cross-section shapes of wires, and then proposed the concept of effective porosity for a general mesh structure. Tian et al.6) measured both the pressure loss and heat transfer performance characteristics of brazed woven mesh structures in forced air convection. They evaluated the effect of different cell shapes and different orientations of the structure, and found that the pressure drop is dominated by form drag while solid conduction and fluid convection are both important for the heat transfer.

Furthermore, it was found that for a fixed surface area density there exists an optimal porosity for maximal heat dissipation. For solar energy collection, Kolb et al.2) found that the woven screen matrix yields an improved thermal performance with higher heat transfer rates and

안수환(교신저자) : 경상대학교 해산연구소 기계시스템공학과
E-mail : asw9294@naver.com, Tel : 055-772-9105
오세경, 이명성(대학원생) : 경상대학교 기계시스템공학과
B.K.P Ary : Sepuluh Nopember Inst. Tech., Indonesia

smaller friction losses compared to traditional flat-plate design. They also suggested that a simulation model is needed for optimization design because of the large number of design and operation parameters.

By considering only the conduction of woven screen layers saturated with fluid. Hsu et al.11) studied the effective thermal conductivity of woven screens at the stagnation situation. Ozdemir and Ozgue12) experimentally determined the porosity values for each layer of a woven screen structure, and confirmed that this exponentially damping porosity is necessary in the models in order to count for the sidewall effect. In these models, the effective thermal conductivities were determined either using data from packed bed or from woven screens with fluid convection ignored.

Ebisu13) applied the wire mesh fin to circular finned tube heat exchangers. A good design copper mesh fin heat exchanger using 4 mm-diameter tubes yields approximately 100% higher heat transfer at same pumping power than the conventional fin heat exchanger. And the high heat transfer coefficients of the mesh fin at a tube diameter of 4 to 5 mm, and large surface-to-volume ratio of the mesh fin heat exchanger lead to the high performance.

The attempts were entirely based on a woven screen installed at the whole cross-section of the channel and a woven screen attached on the tube surface. There was no report of previous work on the heat transfer and friction factor in the channel with ribs made of woven screen.

The objective of this study is to measure heat transfer coefficients and friction factors for a transverse parallel woven metal screen rib roughened rectangular channel with spacing (p/e) of 10. The Reynolds number tested are between 23,000 to 58,000.

2. Test section and experimental procedure

Air is ducted in from the blower. The heated test section utilized is detailed in Fig. 1. It has a rectangular cross section of 200 mm(W) x 40 mm(H) and a length of 712 mm(L)passing a long unheated straight rectangular channel of 1.72 m. The connection between the blower and the test setup was made with a flexible high pressure tube to minimize vibration. The channel has an aspect ratio of 5 and a hydraulic diameter of Dh=66.6 mm. A control valve was used to control the flow rate. The left, right and upper walls are made of 5 mm thick plexiglas plates and the bottom wall is made of 1 mm thick copper plate being flush with the surface at the entrance and exit of test section. The 0.1 mm thick stainless foil heater is glued to the bottom of the copper plate with thermal epoxy resin and 60 mm thick pine wood plate is installed below the heater in order to reduce the heat transfer losses to surrounding.

A mixing chamber was located downstream of the test section to stabilized the flow. A pitot tube was placed in the flow measurement section downstream of the mixing chamber at a fixed position to measure the centerline velocity of air in this channel. A continuity equation is used to determine the average air velocity ub, in the rectangular test section. Room temperature was maintained around 22~25℃, relative humidity of air was recorded 40~51%, and Reynolds numbers were varied from 23,000 to 58,000.

The heater could be controlled by a variable transformer which provided a constant heat flux. The power input can be varied by controlling a single phase transformer and measured by measuring the voltage applied to the heater by a digital multi-meter.

The time to reach steady state was less than 60 minutes. Over the ranger of test conditions, the wall-to-bulk fluid temperature difference was between 9℃ and 46℃. Since the turbulence generated by ribs tends to be dominant, the influence of free convection on the heat transfer in these experiments was believed to be negligible. The ribs used are made of plain weave type copper woven screens shown in Fig. 2 and

attached to the heater at which the height of the rib(e) is 5 mm and the pitch between both ribs (p) is 50 mm. The detailed specification and definition of ribs. were given in Table 1 and Fig. 2.

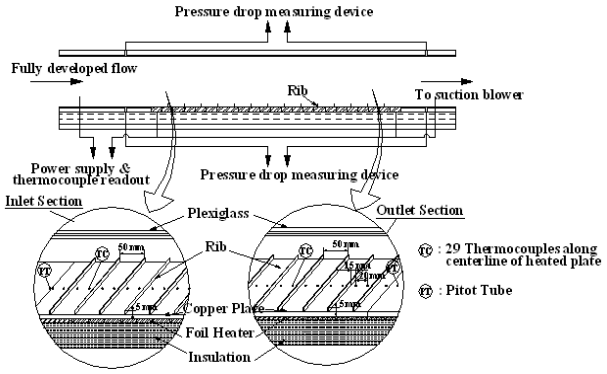

Fig. 1 Details of test section

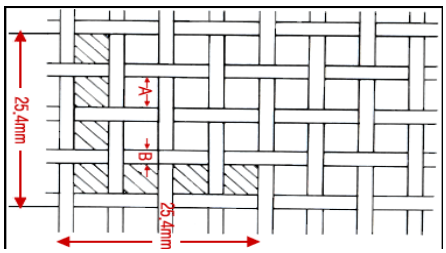

Fig. 2 Definition of woven screen

Ten thermocouples (T type), which were transversed vertically, were used to measure bulk mean air temperature at the exit of the test section. The heat transfer coefficient in this study is based on the smooth area (disregarding the projected area) as the total area.

An exit duct downstream of the instrumented channel is provided to ensure hydrodynamically fully developed conditions. The 29 thermocouples are glued to the copper plateusing an epoxy resin at the centerline. The thermocouple beads are located at 15 mm and 35 mm downstream of each rib. These thermocouples are connected to data acquisition system (DA 100, Yokogawa). The thermocouple beads are carefully embedded into the bottom copper wall and then ground flat to ensure that they are flush with the surface.

All these measurements along the test runs were collected, processed, stored, and analyzed and displayed by a personal computer through the data acquisition system.

Table 1 Woven screen mesh specification

Solid rib	Height (mm)		Thickness (mm)	
	5		1	
Plain weave woven mesh	Type	Mesh	woven diameter, B (mm)	Opening, A(mm)
	A	12	0.6	1.51
	B	10	0.7	1.84
	C	8	0.8	2.37
	D	7	1.2	2.58

Six pressure probes were used to measure pressure drops, and they are located at three positions of top, side, and bottom walls at 100 mm upstream of test section and three positions at 80 mm downstream of test section. Since the pressure taps were located upstream and downstream of actual test section, a correction on pressure drop was performed based on the smooth channel analysis by the micro-manometer(FCO-12, Furness Control Ltd). All of the thermocouples used in this experiment are carefully calibrated against the thermal bath with an accuracy of 0.3℃ or less over the range of operating temperatures. The experimental Reynolds number is evaluated as:

$$Re = \frac{\rho u_b D_h}{\mu} \tag{1}$$

where u_b is a bulk air velocity in a rectangular test section channel. A relation in terms of 1/7th power law velocity profile in a circular tube14) in the circular tube is defined as:

$$V = 0.817\,U \tag{2}$$

where V is the average velocity in the circular tube, and U is the centerline velocity. A continuity equation is used to determine the bulk mean air velocity u_b in the test section as:

$$u_b A_t = V A_f \tag{3}$$

where, A_t and A_f denote the cross sectional area of test section in the rectangular channel and flow measurement section in the circular channel, respectively. The friction factor for fully developed

flow in a rectangular channel can be defined in terms of the dimensionless channel length normalized by the hydraulic diameter D_h, pressure drop ΔP, and bulk mean velocity u_b as follows:

$$f = \Delta P/[4(L/D_h)(\rho u_b^2/2)] \quad (4)$$

The channel average friction factor(f_{avr}) is the average of the top wall friction factor(f_t), the side wall friction factor(f_s), and the bottom wall friction factor (f_b) as follows:

$$f_{avr} = [W(f_t + f_b) + 2Hf_s]/(2W + 2H) \quad (5)$$

The channel average friction factor(f_{avr})is normalized using the friction factor for a fully developed turbulent flow in a smooth circular channel proposed by Blasius15).

$$f_{avr}/f_{ss} = f_{avr}/(0.079Re^{-0.25}) \quad (6)$$

Since the channel of test section is not perfectly insulated, it tends to lose the heat through the wall. Therefore, the heat loss calibration tests were performed before taking measurements. In the still air, there are only two main mechanisms of heat loss: radiation and conduction. Since the heat loss by radiation is much lower than by conduction, therefore, in this study the heat loss by radiation is negligible16). The heat lost through the conduction under a certain operating condition can be indirectly calculated by putting a small amount of power into the flux heater while the test section is maintained in still air condition and its interior is filled with fiber-glass. The heat supplied at a steady state is equal to the heat leakage through the external insulation. This test is conducted for two steady state temperatures, corresponding to the lowest (on the backside of the bottom wall) and highest temperature of the insulation material. Typical heat loss values are to the tune of 3~5% of the total heat supplied.

The local heat transfer coefficient (h) is calculated from the net heat transfer rate per unit surface exposed to the cooling air, the local wall temperature (T_w) and the local bulk mean temperature (T_b) as follows:

$$h = \dot{Q}[A(T_w - T_b)] \quad (7)$$

where A is the total heat transfer area heated wall. $\dot{Q}$ is the net heat transfer rate as follows:

$$\dot{Q} = \dot{Q}_p - \dot{Q}_{loss} \quad (8)$$

The local Nusselt number is defined using the local heat transfer coefficient and the hydraulic diameter D_h for the rectangular channel:

$$Nu = hD_h/k_{air} \quad (9)$$

The channel average Nusselt number (Nu_{avr}) is normalized by the Nusselt number(Nuss) for fully developed turbulent flow in a smooth circular tube correlated by Dittus-Boelter15) as:

$$Nu_{avr}/Nu_{ss} = \sum(Nu_{local})/(0.023Re^{0.8}\mathrm{Pr}^{0.4}) \quad (10)$$

The experimental uncertainties were estimated using the procedure outlined by Kline and McClintock17). It is found that the uncertainties of Reynolds number, friction factor and Nusselt number were 2.5%, 9.5%, and 7.7%, respectively.

3. Results and discussion

The local Nusselt number is plotted with x/Dh in Fig. 3 for various tested Reynolds numbers at case of woven screen rib A having woven wire diameter of 0.6 mm and screen opening of 1.51 mm.

Greater Re values demonstrate greater Nusselt numbers - a trend documented extensively in literature. This is possibly due to the stronger secondary flow traveling along the rib impinging on the smooth surface at greater Re.

At the entrance of test section, the graph of Nusselt number has a peak. It is supposed to the fact that the thinner thermal boundary layer is experienced at the entrance.

Qualitatively, Nusselt numbers become greater at the exit of test section. It is because the temperatures of the wall become abruptly lower after test section with the foil heater; Therefore, the axial heat conduction might be introduced at the exit.

Figs. 4 and 5 indicate the local Nusselt number variations for the woven screen rib B having woven diameter of 0.7 mm and opening of 1.84 mm and the woven screen rib C having woven diameter of 0.8 mm and opening of 2.37 mm. The tendencies are qualitatively similar with the rib A; However, these have higher pronounced effects on heat transfer than the rib A. It might be attributed to the fact that, in the range studied, the woven diameter has more pronounced effect on obstruction for fluid to penetrate into the woven screen opening.

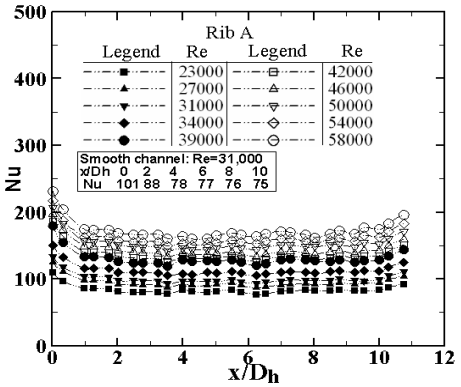

Fig. 3 Local Nusselt number for rib A

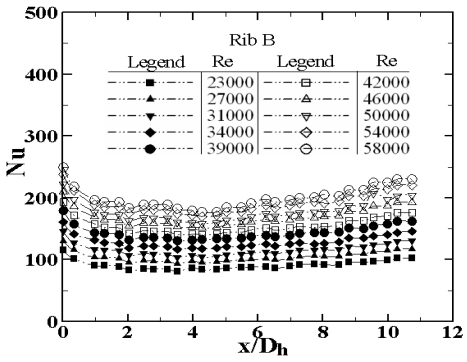

Fig. 4 Local Nusselt number for rib B

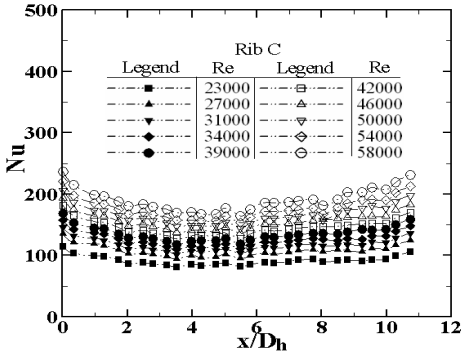

Fig. 5 Local Nusselt number for rib C

Therefore, the ribs B and C produce stronger secondary flows – and this secondary flow induces more turbulence – and therefore more heat transfer. Though the woven diameter of the rib C is a little greater than the rib B, the woven opening of the rib C is much greater than the rib B. This leads that the increase in the Nusselt number of the rib C is a little less than the rib B.

Fig. 6 represents local Nusselt number for the woven screen rib D with woven diameter of 1.2 mm and opening of 2.58 mm.

The local Nusselt numbers of the rib D are greater than the ribs A, B and C. The combined effects of woven diameter and opening can be appreciated by comparing Figs. 3~6.

With the Reynolds number varied, Fig. 7 addresses the effect of the solid rib with e/Dh =0.75 on the Nusselt number.

For a comparison, the work of Rallabandi, et al.18) is included, at which experiments to determine heat transfer coefficients and friction factors are conducted on stationary 45o parallel rib roughened square channel. Reynolds number is 30,000. The ribs have rounded edges and the rib height (e) to hydraulic diameter (Dh) ratio (e/Dh) is 0.094; spacing (p) to height ratio (p/e) is 10.

Qualitatively, these curves in Fig. 7 agree with the observation by Rallabandi, et al.18) – the repeated ribs introduce a local lump at intermediate values of x/Dh of 5.2. The local lumps in Figs. 3-7 are placed around x/Dh=1~2 downstream of Rallabandi, et al.18)

It is because, when the shorter rib (e/Dh=0.075) is introduced, the later regime shifts from a purely skin friction case to a case dominated by form-drag. When used with gases whose Prandtl numbers are close to unity, the relation of the heat transfer coefficient to the friction loss is in fair agreement with the Reynolds analogy19).

The increase in the heat transfer coefficient was seen in the order of solid rib, rib D, rib B, rib C and rib A in the range studied.

The measured friction factors are shown in Fig. 8. The flow encounters obstructions (solid ribs) and forms separation zones immediately

downstream of the solid ribs, which induces drag on the test section, and therefore a pressure drop in the flow. Solid ribs also trip the boundary layer – necessitating the development of a new boundary layer after the flow reattaches. This results in thinner boundary layers and therefore, greater friction factors. However, the woven screen rib has less pronounced effect of obstruction on the fluid flow. Clearly, the combined effects of woven mesh, woven diameter, and woven opening introduce the additional pressure drop. The magnitude of the increase in the friction factor is in the order of solid rib, rib D, rib B, rib C, and rib A.

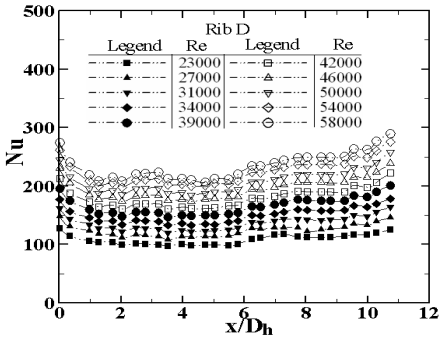

Fig. 6 Local Nusselt number for rib D

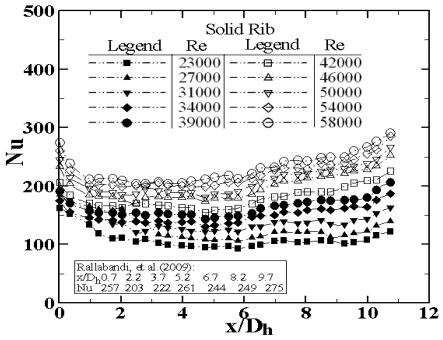

Fig. 7 Local Nusselt number for solid rib

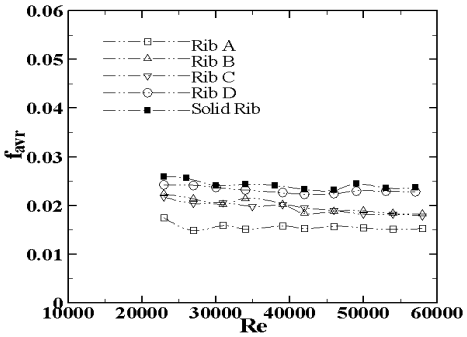

Fig. 8 Friction factors

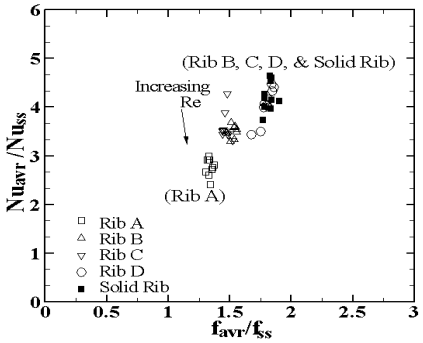

Fig. 9 Heat transfer enhancementagainst friction factor penalty.

Fig. 9 compares the ribbed-wall-average heat transfer enhancements (Nuavr/Nuss) on the ordinate with (favr/fss) on the abscissa. This graph shows the deterioration in performance (decreasing Nuavr/Nuss and keeping almost constant favr/fss or a little decreasing favr/fss) as Re increases – This trend has been extensively shown in literature. The solid rib produces the greatest Nuavr/Nuss and favr/fss because the flow encounters the greatest obstruction and forms the thinnest boundary layer.

4. Conclusions

In this study, the heat transfer and friction characteristics of woven screen ribs have been studied and compared with solid ribs. Detailed regionally heat transfer enhancement and friction factors ratio have been presented for the range of 23,000 to 58,000. The major findings are as follows:

1) The solid rib produces stronger secondary flows – and this secondary flow induces greater turbulence – and therefore greater heat transfer than the woven screen rib.

2) The magnitude of the increase in the friction factor is in the order of solid rib, rib D, rib B, rib C, and rib A.

3) The solid rib produces the greatest Nuavr/Nuss and favr/fss.

References

1. U. Bin-Nun, D. Mantitakos, 2004, "Low Cost

and High Performance Screen Laminate Regenerator Matrix", Cryogenics, Vol. 44, pp. 439-444.
2. A. Kolb, E. R. F. Winter, R. Viskanta, 1999, "Experimental Studies on a Solar Collector with Metal Matrix Absorber", Solar Energy, Vol. 65, pp.91-98.
3. N. S. Tharur, J. S. Saini, S. C. Solanki, 2003, "Heat Transfer and Friction Factor Correlations for Packed Bed Solar Air Heater for a low Porosity System", Solar Energy, pp. 319-329.
4. P. J. Richards, M. Tobinsons, 1999, "Wind Loads on Porous Structure", J. Wind Eng. Ind. Aerodyn., Vol. 83, pp.455-465.
5. A. Bejan, S. L. Kim, A. I. M. Morega, S. W. Lee, 1994, "Cooling of Stacks of Plates Shielded by Porous Screens", Int. J. Heat Fluid Flow, Vol. 16, pp. 16-24.
6. J. Tian, K. Kim, T.J. Lu, H. P. Hodson, D. T. Qucheillant, D. J. Sypeck, H. N. G. Waley, 2004, "The Effects of Topology upon Fluid-flow and Heat Transfer within Cellular Copper Structures", Int. J. Heat Mass Transfer, Vol. 47, pp. 3171-3186.
7. T. Kim, 2003, "Fluid Flow and Heat Transfer in a Lattice Frame Material", Ph.D. thesis, Dpt. of Mech. Engineering. Univ. of Cambridge.
8. S. Ergun, 1952, "Fluid flow through Packed Column", Chem. Eng. Prog., Vol. 48, pp. 89-94.
9. J. C. Armour, J. N. Cannon, 1968, "Fluid Flow through Woven Screens", AIChE J. Vol.14, pp. 415-421.
10. J. R. Sodre, J. A. R. Parise, 1997, "Friction Factor Determination for Flow through Finite Woven Mesh Woven Screen Matrices", ASME J. Fluid Eng. Vol. 119, pp. 847-851.
11. C. T. Hsu, K. W. Wong, P. Cheng, 1996, "Effective Stagnant Thermal Conductivity of Woven Screen", J. Thermophysics, Vol. 10, pp. 542-545.
12. M. Ozdemir, A. F. Ozgue, 1997, "Porosity Variation and Determination of REV in Porous Medium of Screen Meshes", Int. Commun. Heat Mass Transfer, Vol. 24, pp. 955-964.
13. T. Ebisu, 1999, "Development of New Concept Air-cooled Heat Exchanger for Energy Conservation of Air-conditioning Machine, in Heat Transfer Enhancement of Heat Exchangers", S. Kakac et al. Eds., Kluwer Academic, Dordrecht, pp. 601-620
14. W. M. Kays and A. L. London, 1964, Compact Heat Exchanger, McGraw Hill Inc.
15. W. M. Kays and M. E. Crawford, 1990, Convective Heat and Mass Transfer, 2nd ed., McGraw Hill Inc., NewYork.
16. E. M. Micheal, 2003, Radiative Heat Transfer, Academic Press, San Diego, pp. 162-189.
17. S. J. Kline and F. A. McClintock, 1953, "Describing Uncertainties in Single Sample Experiments", Mechanical Engineering, Vol. 75, pp.3-8.
18. A. P. Rallbandi, N. Alkhamis, J. C. Han, 2009, "Heat Transfer and Pressure Drop Measurements for a Square Channel with 45 deg Round Edged Ribs at High Reynolds Numbers", Proc. ASME Turbo Expo 2009: power for land, sea and air, Orlando, GT2009-59546.
19. J. P. Holman, 1997, Heat transfer, 8th ed., McGraw Hill, pp. 218-282.